



TECHNISCHE  
UNIVERSITÄT  
WIEN

BACHELOR THESIS

**The application of GPR for the modeling of ERT data and the  
evaluation of resolution for different electrode configurations**

TU Wien

Department of Geodesy and Geoinformation

Research Group Geophysics

Performed by

Antonio Marco Monteagudo

Enrolment number: 1429697

Under supervision of

Dipl.-Ing. Ingrid Schloegel

Univ. Ass. Dr.rer.nat. Adrián Flores Orozco

Vienna, 6 July 2015

## TABLE OF CONTENT

MOTIVATION .....	3
INTRODUCTION .....	4
THEORIC FUNDAMENTALS .....	5
ELECTRICAL PROPERTIES OF SUBSURFACE.....	5
Electrical Resistance .....	5
Electrical Resistivity .....	5
Electrical Conductivity .....	5
Apparent resistivity.....	6
Dielectric constant .....	7
GPR.....	7
Introduction.....	7
Filtering of GPR datasets.....	8
ERT .....	9
Introduction.....	9
Four electrode array .....	9
MODELING DATA.....	11
INTRODUCTION .....	11
FORWARD MODELING IN GPR .....	11
FORWARD MODELING IN ERT .....	12
INVERSE MODELING IN ERT .....	12
GPR AND ERT MODELS .....	13
CASE 1 .....	13
CASE 2 .....	15
CASE 3 .....	17
FIELD DATA .....	20
INTRODUCTION.....	20
MESUREMENT INSTRUMENTS .....	21
ACQUISITION DATA .....	22
RESULTS .....	23
GPR .....	23
ERT .....	25
APPLICATION IMPROVEMENT .....	26
CONCLUSIONS .....	30
BIBLIOGRAPHY.....	31

## **MOTIVATION**

Nowadays the use of geophysical methods like Ground Penetrating Radar (GPR) and Electrical Resistivity Tomography (ERT) are common tools for underground exploration and engineering applications. However, common field procedures decide upon one method or another to reduce acquisition time. The aim of this thesis is to demonstrate the improvement of the imaging results using both techniques combined over a single method. Use GPR and ERT in a complementary manner is relatively recent due to the complexity of solving the inversion data models of ERT. Computing advances allow processing the inversion of ERT datasets faster and easier and with the interpretation of GPR data helps significantly final results.

## INTRODUCTION

This thesis aims at improving the acquisition of ERT measurements taking into account existing information and GPR results. To achieve this, extensive numerical examples were performed using GPR results for the modeling of ERT datasets for different electrode configurations. Further inversion of the datasets permitted to evaluate the resolution of the electrical images.

My results demonstrate the benefits of working with the combination of GPR and ERT. If we analyze both methods independently they provide information of special changes in the electrical properties of the subsurface. From GPR it can extract qualitative information interpreting the radargrams and from ERT it can obtain quantitative information analyzing the electrical properties from datasets.

The methodology investigated in this thesis is to use GPR results for the digitalization of electrical models. Such electrical models could be used in the forward modeling of ERT datasets –i.e., to investigate the resolution of inversion results for different configurations-, but also to improve the interpretation of the resulting electrical parameters. Is hard to interpret the inverse imaging of ERT without extra information, for this reason the use of GPR results improve the interpretation of electrical imaging.

With the combination of both techniques it is intended to obtain qualitative and quantitative information of the subsurface –i.e., water content, geophormological structures, hydrogeological parameters, etc. -. The interpretation of radargrams, as obtained from GPR, gives qualitative information about buried structures, whereas ERT gives quantitative information about the resistivity of electrical current after the inversion data.

## THEORIC FUNDAMENTALS

### ELECTRICAL PROPERTIES OF SUBSURFACE

This chapter describes the electrical properties of the subsurface and the physical principles of the GPR and ERT methods. To better understand the application and interpretation of GPR and ERT measurements it is necessary to describe some electrical concepts and the basic principles of the GPR and ERT method.

#### Electrical Resistance

Based on the Ohm's Law [1], the electrical resistance ( $R$ ) of a material is the opposition to the flow of a current through a conductor, as showed in equation (1). It can be described as the relation between the electrical potential difference ( $V$ ) and the current passing through a resistance ( $I$ ). The unit of electrical resistance is the Ohm ( $\Omega$ ).

$$R = \frac{V}{I} \quad (1)$$

#### Electrical Resistivity

The resistivity is the electrical property of a material that determines the resistance of a piece of given dimensions (Figure 1). Consider a cylindrical sample of material of length  $L$  (m), resistance  $R$  ( $\Omega$ ) and cross-sectional area  $A$  ( $m^2$ ). The units of resistivity is measured are  $\rho$  ( $\Omega \cdot m$ ) [1].

$$\rho = \frac{RA}{L} \quad (2)$$

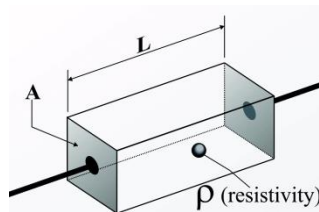


Figure 1. Schema of electrical resistivity

#### Electrical Conductivity

Electrical conductivity is the ability of a material to conduct (transmit) an electrical current [1]. Generally conductivity is expressed in either Siemens per meter (S/m) or, more commonly, milliSiemens per meter (mS/m). Electrical conductivity is the inverse of resistivity and it can be expressed by the equation (3).

$$\sigma = \frac{1}{\rho} \quad (3)$$

Electrical current can be conducted in the materials of the subsurface through three different mechanisms: electrolytic, electronic and interfacial conduction [4].

- Electrolytic conduction occurs by the movement of ions within an electrolyte. This is the dominant mode of conduction in soils and rocks.

- In Electronic conduction the current is carried by electrons. For most rocks (which are near perfect insulators) such conduction will not occur, but if the rock contains metallic minerals (which act as conductors) this can contribute to the overall conductivity.
- Grain surface properties can give rise to a so called interfacial conductivity (which for interfacial conduction). This conductivity originates within the electrical double layer (EDL) which is formed at the interface between the electrolyte and grain surfaces. Interfacial conductivity is complex (i.e. it has a real and imaginary part)

Archie's law (1942) states that electrical conductivity of sedimentary rocks ( $\sigma_0$ ) is related to porosity ( $\phi$ ), fluid conductivity ( $\sigma_f$ ) and saturation (S), as it is shown in equation (4).

$$\sigma_0 = \frac{\phi^m}{a} * \sigma_f * S^n \quad (4)$$

a, m and n are empirical constants:  $0.5 \leq a \leq 2.5$ , cementation exponent  $1.3 \leq m \leq 2.5$  and n roughly 2. The units of the electrical conductivity are measured generally in Siemens per meter.

It is important to say that Archie's law is only valid for soils and rocks without clay minerals. This is due to the fact that clayed minerals has an elevated surface conductivity and turn the formula unstable. For this reason the formula was rewritten and adds the surface conductivity ( $\sigma_s$ ) value as it is shown in equation (5). This formula it is called extension of Archie's law (1960).

$$\sigma_0 = \frac{\phi^m}{a} * \sigma_f * S^n + \sigma_s \quad (5)$$

### Apparent resistivity

Over homogeneous isotropic ground the resistivity will be constant for any current and electrode arrangement, which will speak in the following sections. If the ground is inhomogeneous, however, and the electrode spacing is varied, or the spacing remains fixed while the whole array is moved, then the ratio will, in general, change. This results in a different value of resistivity for each measurement. The magnitude is intimately related to the arrangement of electrodes. The equation (6) shows this measured quantity and this is known as the apparent resistivity [2]:

$$\rho_a = \frac{V}{I} k \quad (6)$$

Where:

V: potential difference.

K: geometrical factor.

I: current intensity.

## Dielectric constant

The electromagnetic wave velocity in a non-magnetic (relative magnetic permeability  $\mu_r = \mu/\mu_0 = 1$ ) medium is given approximately by the formula shown in equation (7).

$$v = \frac{c}{\sqrt{\epsilon_r}} \quad (7)$$

Where  $c = 3 \cdot 10^8$  m/s is the speed of light in the vacuum and  $\epsilon_r = \epsilon/\epsilon_0$  is the relative electrical permittivity, or dielectric constant. Sometimes the symbol K is also used for dielectric constant [4].

The electric permittivity is per definition higher than zero. Even in vacuum, the permittivity, takes on a finite value of  $8.85 \times 10^{-12}$  F/m (Farads per meter). The explanation for this lies in the field of quantum electrodynamics and is far beyond the scope of this thesis for geophysical measurements.

It is often more convenient to deal with a dimensionless term called relative permittivity or dielectric constant, K. The relative permittivity is the ratio of material permittivity to the permittivity of a vacuum [3].

$$K = \frac{\epsilon}{\epsilon_0} \quad (8) \quad \epsilon_0 = \text{Vacuum permittivity } (8,85 \times 10^{-12} \text{ F/m})$$

For most dry geological materials, such as sand, gravel, and crystalline rock, the dielectric constants varies roughly in the range  $3 \leq \epsilon_r \leq 8$ . Water has an anomalously large dielectric constant of  $\epsilon_r \sim 81$  due to the high polarizability of the water molecules in the presence of a high frequency applied electric field. Thus, water-bearing rocks have significantly higher dielectric constants ( $\epsilon_r \sim 10 - 30$ ) than dry rocks of the same lithology. Hydrocarbons such as oil and gas have low values of dielectric constants, on the order  $\epsilon_r \sim 1 - 2$ . The dielectric constant and wave velocity of common geomaterials at 100 MHz is listed in Table 1 [4].

MATERIAL	DIELECTRIC CONSTANT	VELOCITY (mm/ns)
Air	1	300
Freshwater	80	33
Seawater	80	33
Dry sand	3-5	120-170
Saturated sand	20-30	55-60
Limestone	4-8	100-113
Clay	5-40	85-170
Granite	4-6	100-120

Table 1. Dielectric constant and wave velocity of common geological materials at 100 MHz

## GPR

### Introduction

The GPR is based on short electromagnetic pulses with theoretical system based on seismic waves, however GPR uses electromagnetic waves. This system is formed by two antennas one of them is the transmitter and the other one is the receiver. The separation between the transmitter and receiver depends on the chosen frequency. The GPR frequency range goes from 10 MHz to 2 GHz. When a wave travels from transmitter to receiver three phenomena

could occur: 1) the wave reflects in a border of different subsurface material and return to receiver, 2) the wave refracts in the border of the material and go on deeper until it reflects on another border, 3) the wave is adsorpted because the properties of material. In Figure 2 can see the schema of three phenomena exposed[3].

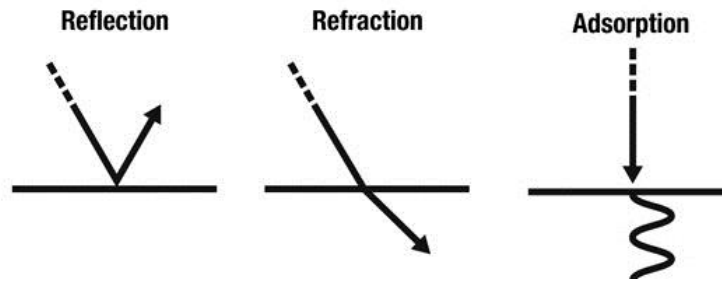


Figure 2. Reflection, refraction and adsorption of electromagnetic wave

The frequency range of GPR antennas goes from 10 MHz to 2 GHz, the higher frequency the shallower penetration depth and also the higher the frequency the higher resolution, this are two important concepts. It is important to know the depth of investigation in every case to choose the right antenna.

In the range of high frequencies the velocity of electromagnetic wave is given by equation (9) [3].

$$v = \frac{c}{\sqrt{K}} \quad (9)$$

Must be taken into account that when a wave travels through the different materials the phenomena of attenuation occurs. An impulsive signal gets dispersed because its frequency components are attenuated at different rates and travel. The attenuation of a radar wave is given by the equation (10) [3].

$$\alpha = Z_0 \cdot \frac{\sigma}{2 \cdot \sqrt{K}} \quad (10)$$

Where:

$\alpha$ : attenuation

$Z_0$ : impedance of free space

$\sigma$ : conductivity

K: dielectric constant

### Filtering of GPR datasets

Filtering it is a useful process in GPR to improve the radar visualization and show better results hidden by the noise of higher frequencies. The software used to filter the profiles is Reflexw. The filters used for this thesis are [7]:

Background removal: It is a process that performs the subtraction of an averaged trace defined by user. The user has to define the range of depth which applies the filter. It is commonly used to remove the direct wave. To process the profiles of this thesis is going to be selected the whole range as parameter of the filter.

Bandpass frequency: It is a process that works on each trace independently. Usually the receivers of radar collect frequencies up and down the main frequency of antenna and this filter it is used to remove this noise from the radargram.

Energy decay: As the amplitude of the signal decays with the greater travel time energy decay is applied to gain the deeper signals. That process works in each trace independently and applies a gain curve in the time direction.

## ERT

### Introduction

ERT it is an electrical method based on a four electrode array. The electrodes could be fixed in ground or in boreholes. From the four electrode array, two of them are used to inject a direct current to subsurface and the other two measures the potential difference generated by the current injection. In this study it is going to analyze two different types of arrays: Wenner and Dipole-Dipole in a Skip configuration.

### Four electrode array

Historically, a number of four-electrode configurations have proven popular used for a wide range of applications of geophysics. As we describe below, computer-controlled configurations of hundreds of electrodes are now routinely deployed (Locke, 1999). Nevertheless it remains worthwhile to briefly discuss a few of the traditional four-electrode configurations in order to gain insight into the capabilities of the resistivity method and to explore the advantages and disadvantages of the various electrode configurations in terms of depth penetration, lateral resolution, ease of deployment, and signal-to-noise ratio.

The Wenner array configuration (Figure 3) spread the electrodes uniformly spaced in a line.

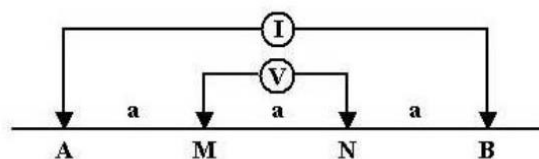


Figure 3. Wenner array electrodes disposition

There is a fixed separation of  $a$  between adjacent electrodes, with the potential electrodes MN placed inside the current electrodes AB. The apparent resistivity is computed based on the geometrical factor. It is easy to see that the geometric factor for the Wenner array is:

$$k = 2\pi a \quad (11)$$

The penetration depth of the Wenner array depends on the spacing  $a$ ; the larger its value, the deeper the penetration. In simple terms, as the spacing between the injection and withdrawal electrodes increases, electric current is driven mainly deeper into the subsurface. The Wenner array is quite effective at mapping lateral contrast in resistivity within the depth of penetration. The array is moderately easy to deploy as the trailing electrode can be leapfrogged to the front as the configuration is advanced along the profile. This means that only one electrode movement is required per measurement. Signal-to-noise ratio is generally good since the potential electrodes MN are located in the central part of the array.

In this thesis we will use the dipole-dipole skip configuration than is based on the classical dipole-dipole configuration, to understand better this configuration first is going to be explained the dipole-dipole configuration. As we can see in Figure 4 the current electrodes AB and the potential electrodes MN have the same spacing  $a$  but the two pairs are widely separated by a distance  $na$ , where  $n \gg 1$ . This a factor changes in every skip test [2].



Figure 4. Dipole-Dipole array electrodes disposition

The geometric factor for the dipole-dipole array is

$$k = \pi n(n + 1)(n + 2)a \quad (12)$$

In the dipole-dipole skip configuration the current electrodes stays fixed and the potential electrodes moves along the line measuring the potential difference. When all the line is measured the current electrodes moves to the next position and the potential electrodes take measurements as it can observe in Figure 5. The skip in the dipole-dipole configuration is the number of electrodes you leave inside the dipoles, this means that the length of dipoles increase.



Figure 5. Dipole-Dipole Skip array disposition

## MODELING DATA

### INTRODUCTION

Modelling is critical to all geophysical methods. One can simulate the system behavior from excitation through to the response which would be observed or measured. Modelling or simulation enables quantitative predictions of responses leading to both a better fundamental understanding and a sound basis for interpretation

- Understanding of physical behavior and quantifying response;
- providing performance requirements for design of measuring instruments;
- predicting response and sensitivity to parameter changes;
- optimizing survey design;
- understanding how to process data to extract information;
- enabling interpretation at a variety of levels of complexity;

In summary, modelling underpins translation of geophysical observations into useful information [3].

### FORWARD MODELING IN GPR

The forward modeling in GPR starts planning a layered model with geometric characteristics. We need to know the total length of the section which wants to model, the depth of the profile and the depth of the different model layers. Once we have clear the arrangement of the layers in space we will define the electromagnetic properties of the layers raised, that is, establish the values of dielectric permittivity and conductivity. This process will be the input of forward modeling.

The software used in this thesis to make the forward modeling in GPR is ReflexW. The forward modelling in GPR is done using a Finite Difference scheme solving the Maxwell's equations [7]. Of the three different sources that are implemented in software (exploding reflector model, plane wave and point-source) we will use the exploding reflector model and plane wave. The exploding reflector model as well as the plane wave allows the modelling of a complete zero offset section in only one step but with some restrictions [8].

Based on the raised model and the method of Finite Difference we obtain as output one radargram (Figure 6) where the propagation of EM waves to the different geometry is observed and also each wave varies in depth and amplitude.

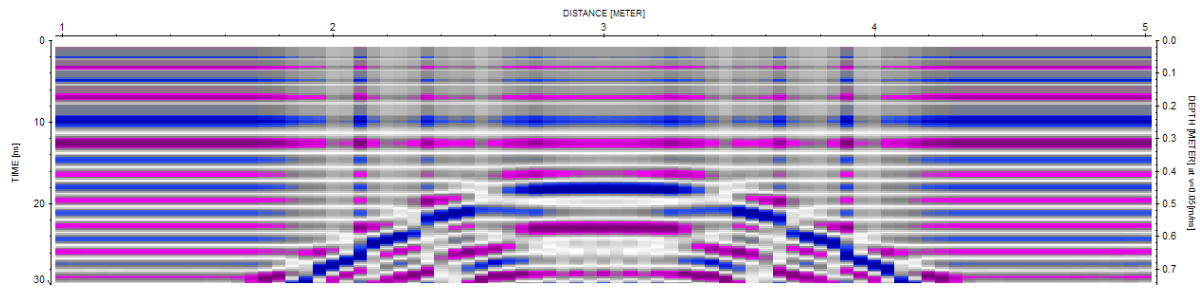


Figure 6. Example of a modeling radargram made with ReflexW

## FORWARD MODELING IN ERT

Forward modeling in ERT consist in determine the measured resistances of subsurface based on resistivities, geometric model and a given configuration. To obtain the electrical potential difference (V) an inverse Fourier transformation is applied [9]. To start the forward modeling it is necessary to know the geometric and electrical characteristics of layered raise model and the electrode array configuration. The units of geometric characteristics are in meters and the input resistivities are given in ohm per meter ( $\Omega \cdot m$ ). The output of the process is a numerical model with the calculated resistances in omh ( $\Omega$ ).

The software used in this thesis is CRMod for geoelectrical modeling. This software calculates the electric potential for each node of the model.

## INVERSE MODELING IN ERT

The inverse modeling in ERT can be described as the process to find the best electrical model of subsurface distribution by a given measured field data. The process starts with a dataset which contain the measured resistances of every node for the set array configuration and end with an electrical image of subsurface with resistivity distribution of values. There are infinites models that explain the same dataset but the point is to find the model that best approach to original measurements with the least root mean square error. Every measure has an associated misfit and to solve the inversion model we will base in the commonly optimization problem function (13). All this process is in more detailed in references [10].

$$\Psi(m) = \Psi_d(m) + \lambda \cdot \Psi_m(m) \quad (13)$$

$\Psi(m)$ : data model misfit

$\Psi_d(m)$ : Chi-squared measure of the data misfit

$\Psi_m(m)$ : model objective function containing the desired model characteristics

$\lambda$ : regularization parameter

The software used in this thesis to make the inversion of dataset is CRTomo. This code needs the position of nodes, the electrode configuration and the file with the distribution of subsurface resistances and the result is a file with the resistivities associated to every node.

## GPR AND ERT MODELS

In the following lines three theoretical models in GPR and ERT will be set with different configurations to observe what their response is. First of all we present three different cases, each one with different geometric and electrical characteristics. The tested configuration for ERT models are: Wenner array and Dipole-Dipole Skip from 0 to 5. The GPR models are made with software ReflexW with the Modelling tool. The inversion of the results has been made with Res2dInv and the plot imaging results have been made by a Matlab algorithm.

### CASE 1

In this first case it has been set a three layers model with the following geometric characteristics:

Layer	X(m)	Depth (m)	Layer	X(m)	Depth (m)
L1	0.00	0.00		0.00	7.00
	48.00	0.00		0.39	6.92
L2	0.00	5.00	L3	4.00	7.17
	5.87	4.07		6.49	6.64
	8.98	2.97		8.73	5.62
	12.34	2.57		10.47	4.60
	16.33	2.28		13.59	4.15
	20.93	2.28		16.20	5.05
	25.42	2.73		16.95	5.78
	28.16	3.14		17.32	7.21
	31.15	3.71		18.94	7.70
	33.26	3.99		20.31	7.58
	38.12	4.11		23.30	7.01
	42.23	3.91		23.67	5.95
	44.47	3.54		24.05	4.97
	47.33	2.61		25.67	4.48
	47.50	2.50		27.91	4.97
	48.00	2.00		29.15	5.58
			32.27	5.87	
			38.37	6.11	
			41.73	5.91	
			46.21	5.62	
			48.00	6.00	

Table 2. Geometric characteristics of Case 1

In Figure 7 we can observe the picture of layered model. The GPR model generated it is longer than the final result to avoid the reflections from the borders. The red window highlights the interested area.

The application of GPR for the modeling of ERT data and the evaluation of resolution for different electrode configurations

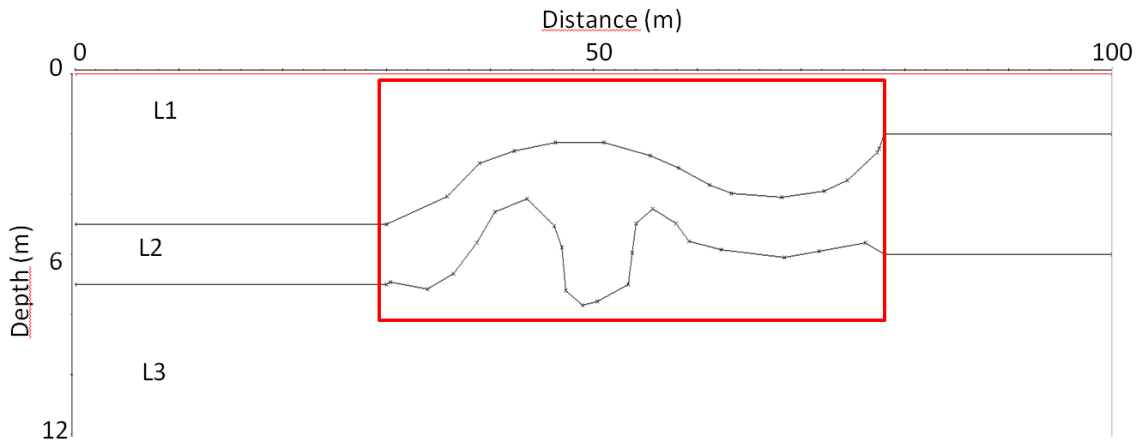


Figure 7. Disposition of layers in Case 1

The table 3 shows the electrical values corresponding to each layer for raised model.

	$\epsilon$	$\sigma$ (S/m)	$\Omega$ (Ohm.m)
L1	15	0,2	50
L2	7	0,001	1000
L3	5	0,003	3333

Table 3. Electrical values of the layers in Case 1.

For this model has been set a frequency of 100 MHz and a range of 300 ns. After the forward modeling of raised model the results are shown below:

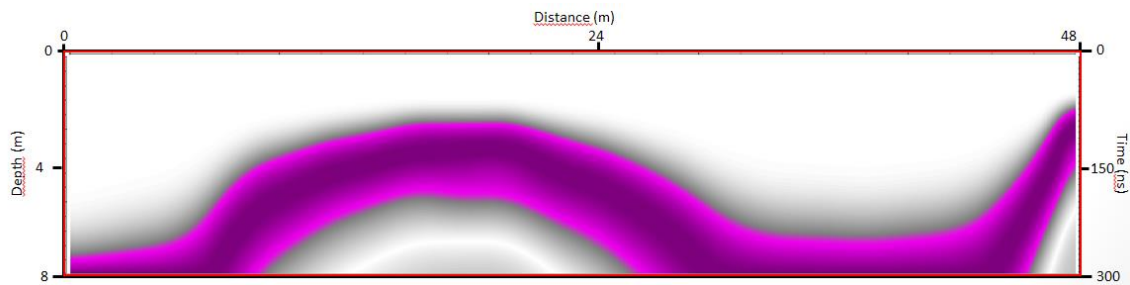


Figure 8. Radargram of model in Case 1

In this model it has looked for the response of the wave to horizontal contrasted layers. The conductivity of the layers decreases with the depth so the signal could not be so good. In this case the first layer it is associated to an average soil mixing clays and sand, the second layer it is associated to a granite layer and the third one it is associated to a hard limestone. As it is observed the forward modeling resolve pretty well the three layer model set, but the depth of the boundary layers it is not right.

Following it can see the ERT inversion results, it has reproduce the same model as GPR with the same geometric and electrical characteristics. The color bar is the same for all the models

and it can see expanded to clarify the interpretation. The first 6 images corresponding to Dipole-Dipole Skip 0 to 5 configuration and the last one to Wenner configuration.

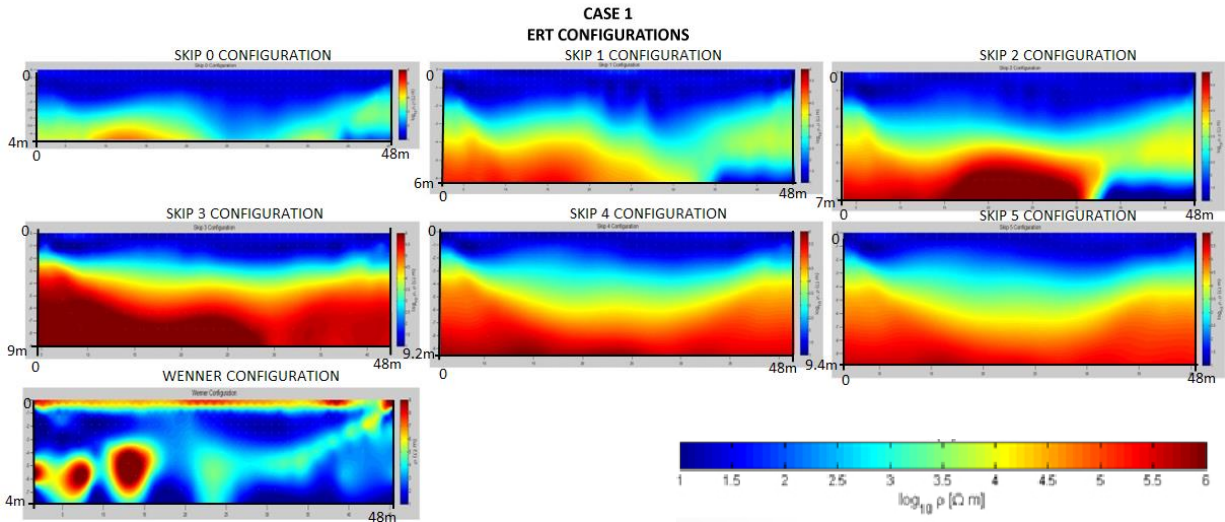


Figure 9. Composition of inverted modeled data with different configurations

As it can observe in the Skip configuration, the higher is the distance between current electrodes the higher depth, but it loses resolution. The point is found the configuration that can solve better the raised model. In this case Wenner configuration is not a good configuration to solve this high resistivity model and the best configuration that solves this is the Dipole-Dipole Skip 2. It can see in this skip the boundary between the three layers and reproduces quite well the form of the layers.

## CASE 2

In this second case it has been set a three layers model with the following geometric characteristics:

Layer	X(m)	Depth (m)	Layer	X(m)	Depth (m)
L1	0.00	0.00	L3	0.00	7.22
	48.00	0.00		6.09	7.21
L2	0.00	5.94		11.77	6.85
	6.81	5.36		15.70	6.32
	10.73	4.92		17.86	5.57
	13.84	4.05		18.94	4.92
	16.55	3.17		20.57	4.40
	18.04	2.61		24.49	3.16
	20.34	1.91		27.88	2.28
	24.67	1.04		35.72	1.02
30.08	0.00	38.97	0.00		

Table 4. Geometric characteristics of Case 2

Just as in the first case the studied area is highlighted in red, in Figure 10 we can see the disposition of the layers and in the Table 5 the electrical values associated.

The application of GPR for the modeling of ERT data and the evaluation of resolution for different electrode configurations



Figure 10. Disposition of layers in Case 2

	$\epsilon$	$\sigma$ (S/m)	$\Omega$ (Ohm.m)
L1	10	0,01	100
L2	7	0,001	1000
L3	5	0,0002	5000

Table 5. Electrical values of the layers in Case 2.

How it can see the raised model is a vertical layered model that conductivity decreases and therefore resistivity increases with the length of profile.

For this model has been set a frequency of 200 MHz and a range of 120 ns. After the forward modelling process, the results are:



Figure 11. Radargram of model in Case 2

In this model it has looked for the response of the wave to around 45 degrees incline contrasted layers. In this case the difference between the first and the second layer is that the contrast is not so high than in first case, this case the second layer is ten times more conductive than the first layer. A geomorphologic interpretation of the layers could be: the first layer it is associated to a non-high wet clay soil, the second layer it is associated to a granite layer and the third one it is associated to a very competent limestone. As it is observed the forward modeling resolve pretty well the contact between layers boundaries and the depth of the boundary layers it is almost right.

The application of GPR for the modeling of ERT data and the evaluation of resolution for different electrode configurations

Following it can see the ERT inversion results, it has reproduce the same model as GPR with a Matlab algorithm with the given resistivities. The first 6 images corresponding to Dipole-Dipole Skip 0 to 5 configuration and the last one to Wenner configuration.

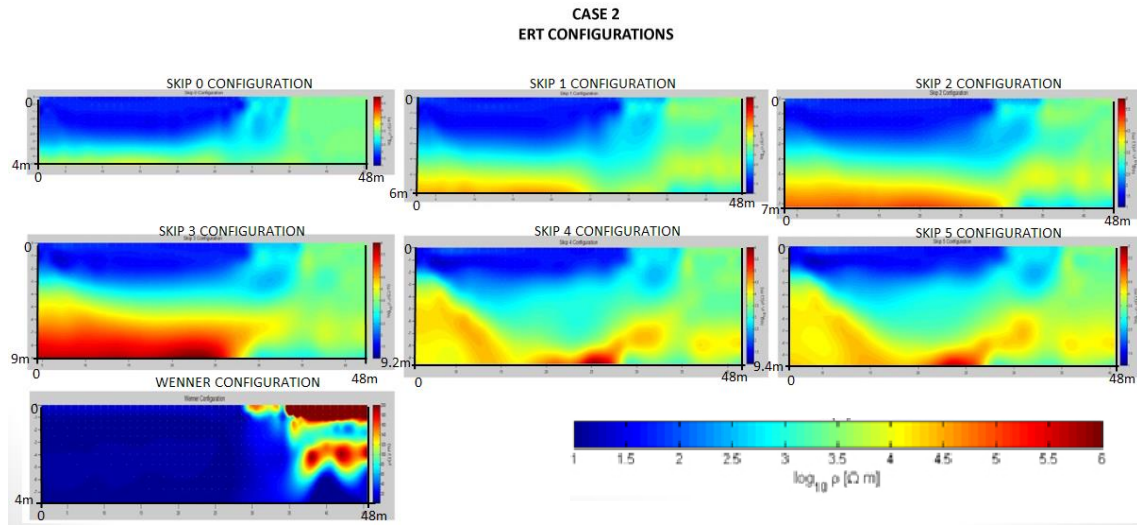


Figure 12. Composition of inverted modeled data with different configurations

In this case Wenner configuration is not a good configuration to solve this inclined model, as it can see the response of the inversion model it is poor. Analyzing the Dipole-Dipole configuration the best configuration that solves this model is the Dipole-Dipole Skip 3. This skip resolves better the model with relation between contact boundary and depth.

### CASE 3

In this third case it has been set a three layers model with the following geometric characteristics:

Layer	X(m)	Depth (m)	Layer	X(m)	Depth (m)
L1	0.00	0.00		0.00	1.20
	48.00	0.00		9.60	1.20
L2	0.00	0.63	L3	20.63	1.10
	4.66	0.69		33.16	0.80
	9.14	0.74		38.42	0.40
	12.87	0.77		41.18	0.40
	17.53	0.80		43.18	0.45
	20.42	0.80		48.00	0.50
	23.77	0.75	Hole	11.20	1.07
	27.69	0.67		11.57	0.81
	30.67	0.61		11.76	0.79
	32.72	0.54		11.88	0.77
35.80	0.47	11.97		0.74	
40.27	0.44	12.53		0.73	
48.00	0.45	12.90		0.72	
		13.05		0.71	
		13.29	0.71		
		13.69	1.03		

Table 6. Geometric characteristics of Case 3

Like in before cases the studied area is highlighted in red, in Figure 13 we can see the disposition of the layers and in the Table 5 the electrical values associated.

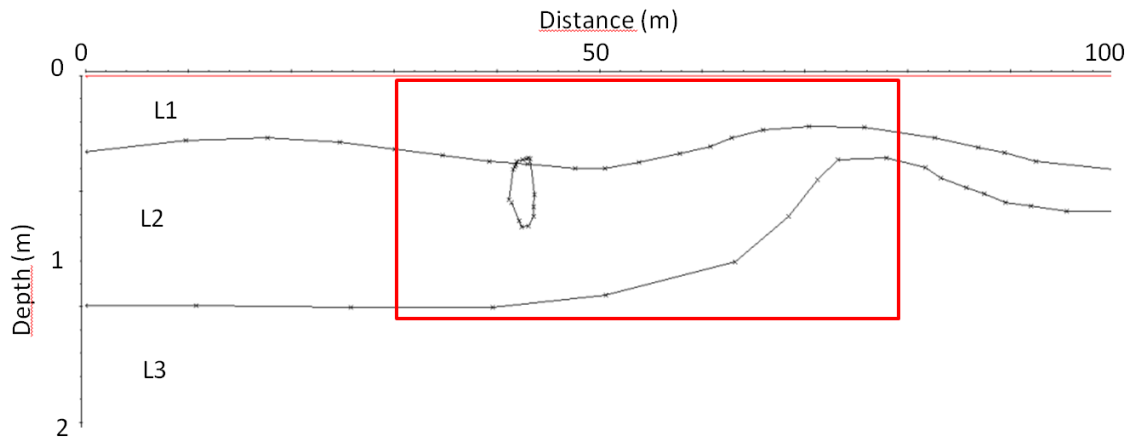


Figure 13. Disposition of layers in Case 3

	$\epsilon$	$\sigma$ (S/m)	$\Omega$ (Ohm.m)
L1	8	0,1	100
L2	6	0,05	1000
L3	5	0,0002	5000
Hole	1	$1.10^{-7}$	$1.10^7$

Table 7. Electrical values of the layers in Case 3.

How it can see the raised model is a horizontal layered model as the first case but in this one it is going to observe the response of methods to a buried hole like a cavity or a hollow. In this model the conductivity decreases and therefore resistivity increases with depth also.

For this model has been set a frequency of 400 MHz and a range of 50 ns. After the forward modelling process, the results are:

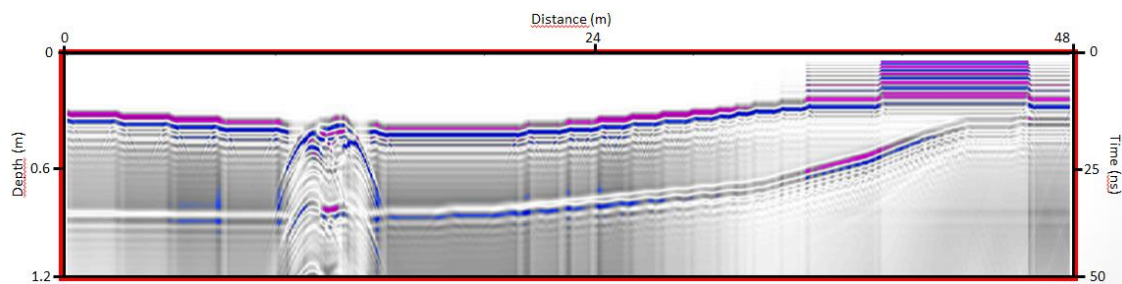


Figure 14. Radargram of model in Case 3

## The application of GPR for the modeling of ERT data and the evaluation of resolution for different electrode configurations

The electrical values of this model are the same than the case 2, but in this case it is going to observe how it is solved a hole of 1 meter of diameter between layer 1 and layer 2. It has changed the boundary conditions to reflecting to improve the signal. As it can see the GPR configuration solves really good the raised model.

Below can be observed the results of the inverted data:

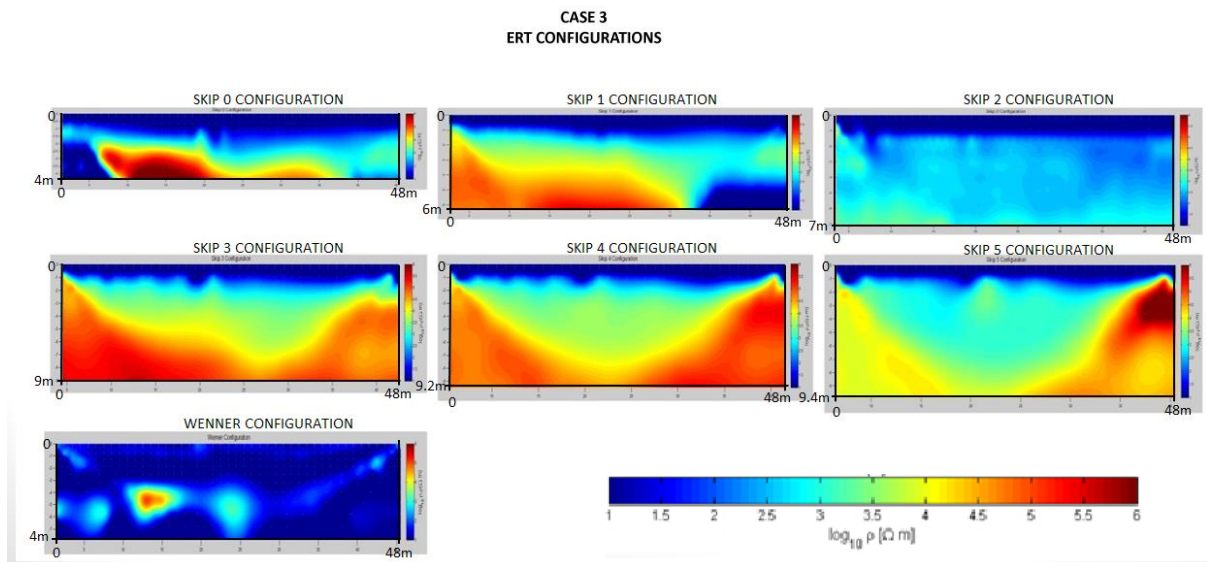


Figure 15. Composition of inverted modeled data with different configurations

At first sight no one configuration solves well the raised model; it cannot observe the boundary contact neither the layer disposition. The reason of this bad solution can be in the raised model because this is a very high resistivity model with high contrast between layers and the energy of the current electrodes remains in the first layer.

## FIELD DATA

### INTRODUCTION

For the aim of this thesis is going to demonstrate that the combination of GPR and ERT methods are effective and it will be possible processing and interpreting field measurements. It will collect data with GPR and ERT equipment and after that it will do an ERT model based on GPR measurements, the results of electrical inversion modeling will compare with the inversion data measurements and will observe how similar both inversions are.

The field data measured in this section took place the 22th of april of 2015 at the north-west of Vienna in the 19<sup>th</sup> district in the area called "Cobenzl". In the pictures below it can be situated:

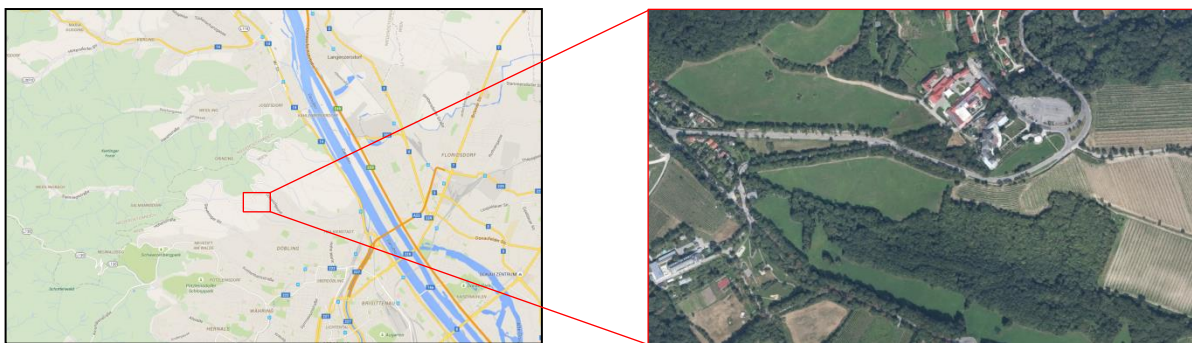


Figure 16. Localization and situation of measurement area (Cobenzl, Vienna)

To make a better idea of what is the nature of subsoil below it is attached a geologic map of this area:

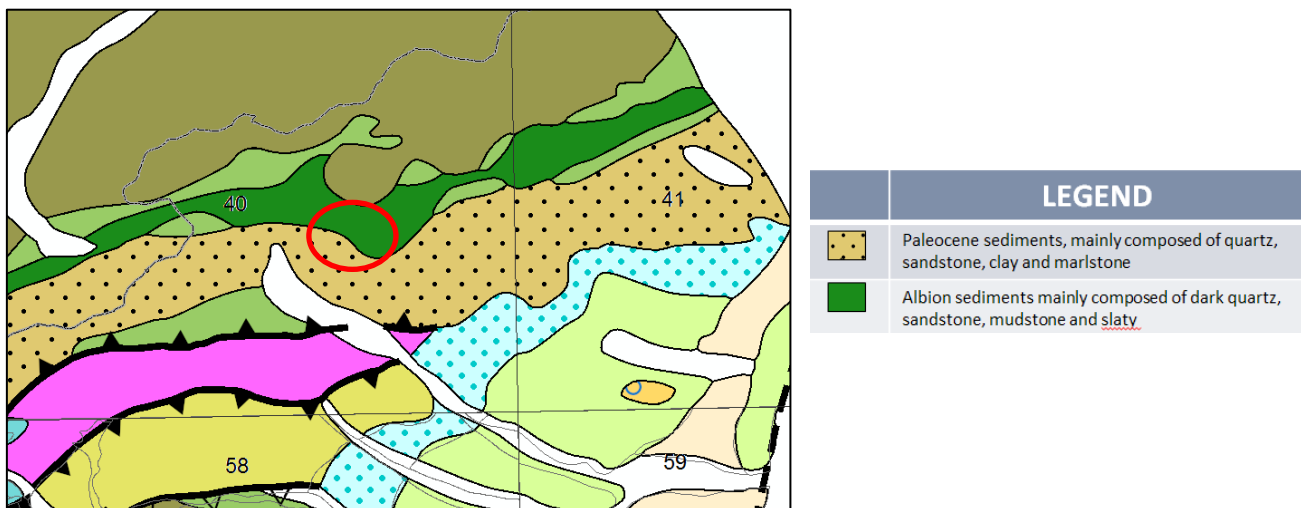


Figure 17. Geology of measurement area

The red circle it is the area where the measurements take place and it can distinguished two different areas. The map legend only shows the geology of the interested area. With this information it could interpret clearly the information from GPR and ERT.

## MESUREMENT INSTRUMENTS

The GPR measurements have been taken with two different antennas, one of 400 MHz and other of 200 MHz, to get information of different depth and have more results for helping in the ERT modeling.

The 400 MHz antenna can penetrate, in better conditions, until 1.80 -2.00 meters and 200 MHz antenna can penetrate until 6.00-7.00 meters, also with favorable conditions.

To record the data was used the SIR-3000 Processor from GSSI Company



Figure 18. SIR-3000 processor.



Figure 19. In left side a picture of 400 MHz antenna and in the right side a picture of 200 MHz antenna.

The ERT measurements have been taken with the Geotom multi electrode resistivity equipment of Geological Survey of Austria. The equipment consists in a resistivimeter which measures the difference of potential, one external laptop to configure the measurements and control all the process, an external battery to produce the energy and a converter to control the quantity of energy.



Figure 20. Image of Geotom multi-electrode equipment.

## ACQUISITION DATA

The field work consisted in take measures of 8 radar profiles with 400 MHz antenna, 6 radar profiles with 200 MHz antenna and 2 electrical resistivity profiles. The electrical measurements were taken with Geological Survey of Austria configuration array, the separation between electrodes was 1,5 meters. The Figure 21 shows the disposition of all profiles.



Figure 21. Disposition of ERT and GPR profiles in study area.

In Table 8 we can observe the length, frequency and direction of GPR profiles.

File Number	Name Protocoll	Lenght	Frequency	Orientation
FILE_003				
FILE_004	HP_I	140	400	E-W
FILE_005				
FILE_006				
FILE_007	QP_I	128	400	S-N
FILE_008				
FILE_009				
FILE_010	QP_II	128	400	N-S
FILE_011				
FILE_012				
FILE_013	HP_II	140	400	W-E
FILE_014				
FILE_015				
FILE_016	HP_I	140	200	E-W
FILE_017				
FILE_018				
FILE_019	QP_II	124	200	S-N
FILE_021				
FILE_022				
FILE_023	QP_I	126	200	N-S
FILE_024				
FILE_025	HP_II	90	200	W-E
FILE_026				
FILE_027	HP_III	80	200	E-W
FILE_028				
FILE_029	HP_IV	100	200	W-E
FILE_030				
FILE_031				
FILE_032	P_V	119	400	E-W
FILE_033				
FILE_034				
FILE_035	P_VI	120	400	W-E
FILE_036				
FILE_038				
FILE_039	P_VII	100	400	E-W
FILE_040				
FILE_041	P_VIII	176	400	NW-SE
FILE_042				

Table 8. Table of GPR profiles characteristics.

## RESULTS

This section shows the results of field data after the process, every radar profile has been processed in the same way; it has applied the same filtering process and gain. For the aim of the thesis it has chosen the HP\_I of 400 MHz and 200 MHz (Table 8) and the parallel electrical profile, although all the results have been filtered and processed. The selected profiles are 140 meters length. This file is selected because compare with the others is the one which show more structures and could be more interesting for the aim of the thesis.

### GPR

The process starts with the 400 MHz profile set with a range of 70 ns. First filter applied is energy decay to emphasize the low amplitude ranges. Below it is shown the file after the process:

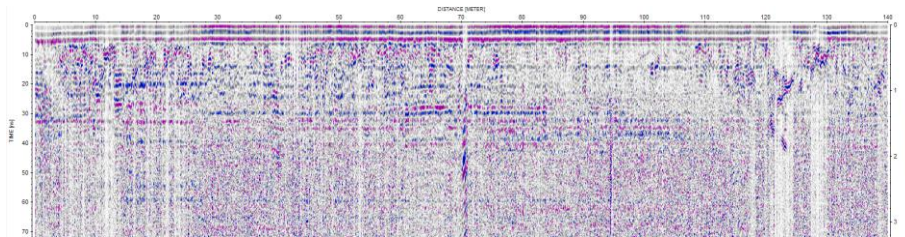


Figure 22. Original 400 MHz GPR radargram.

Afterwards it is make a background removal to remove the direct wave:

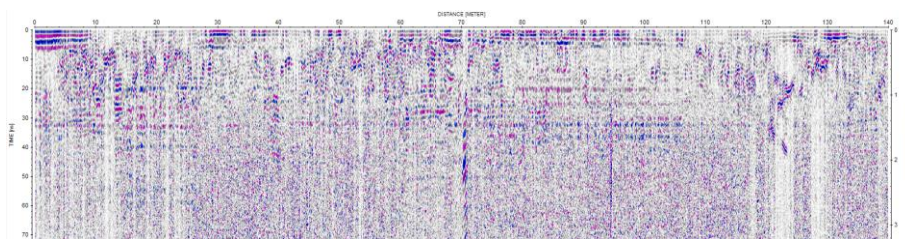


Figure 23. Radargram after background removal filtering.

And, to finish the filtering process it is applied a bandpass frequency to remove all the low and high frequencies received to antenna, the range of values set to this filter is: 300 to low cut off and 500 MHz to upper cut off. The result after the process is shown below:

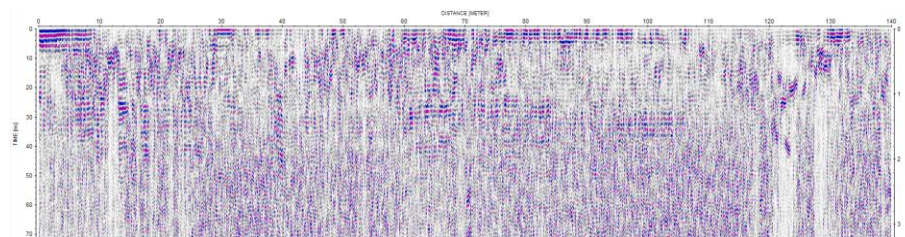


Figure 24. Radargram with Bandpass filter applied.

In order to show the real position of structures and avoid the effect of topography from files it is applied a topographic correction.

# The application of GPR for the modeling of ERT data and the evaluation of resolution for different electrode configurations

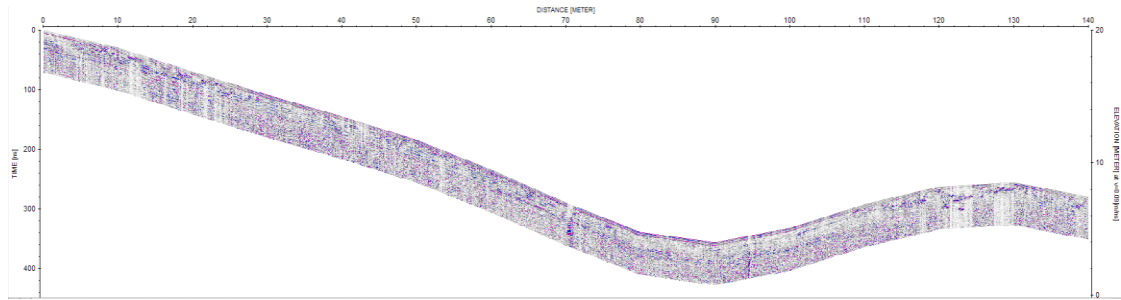


Figure 25. Radargram with topographic correction applied.

The profiles from the antenna of 200 MHz will process in the same way to be able to compare both profiles. This profile is set with a range of 140 ns. Hereafter it is shown the filtering results.

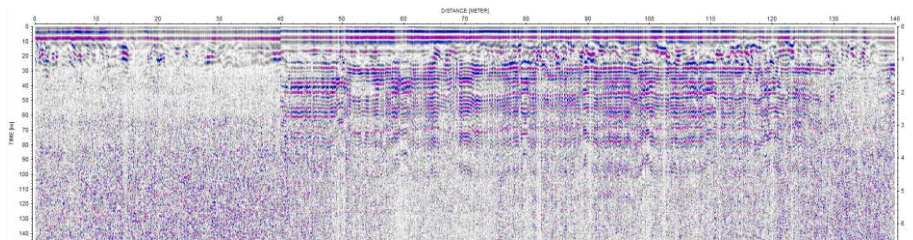


Figure 26. Original 200 MHz GPR radargram.

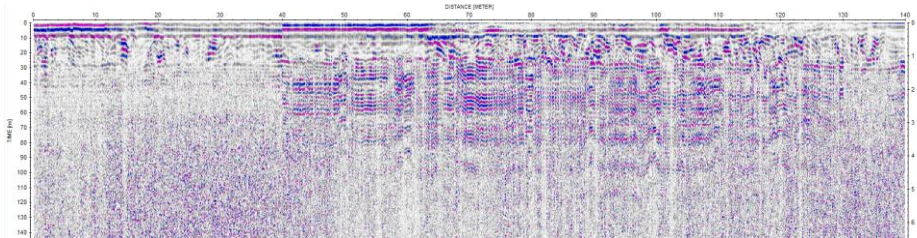


Figure 27. Radargram after background removal filtering.

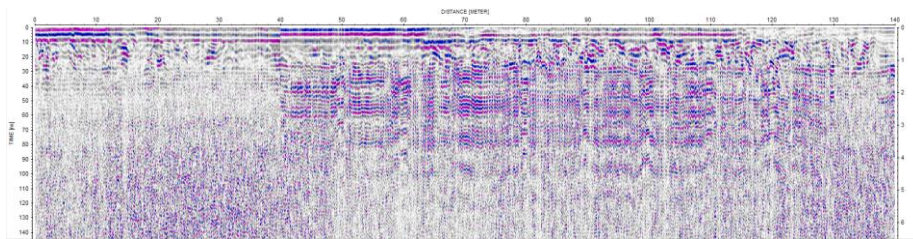


Figure 28. Radargram with Bandpass filter applied with lower cut off of 50 and upper cut off 350.

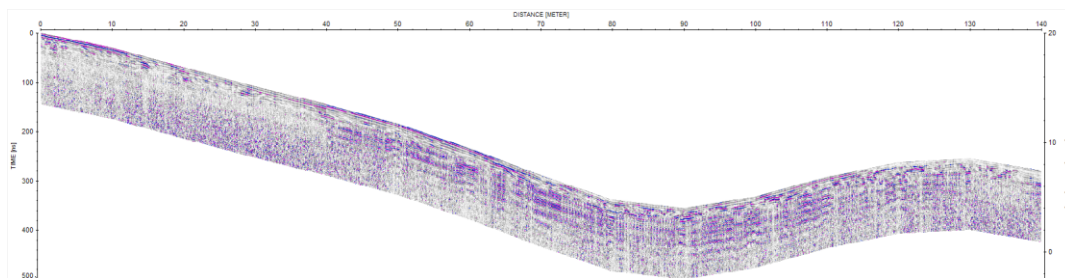


Figure 29. Radargram with topographic correction applied.

## ERT

The electrical field data it is inverted with CR Tomo software. After 3 iterations the RMS error in this model is 5.48%. With this configuration have coverage in the data until 10 meters depth. The results are shown in image below:

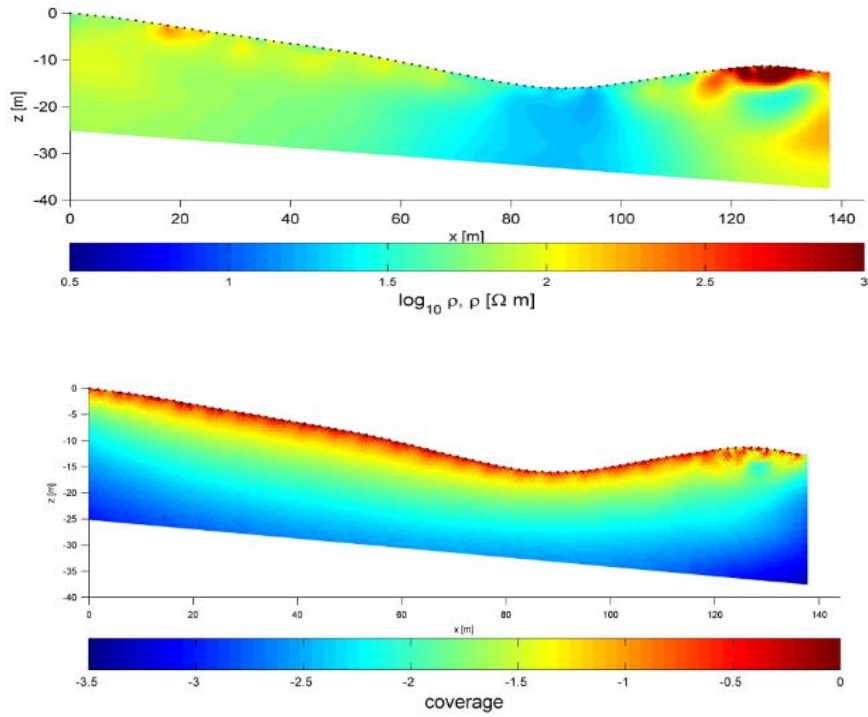


Figure 30. Inversion image of electrical field data.

Figure 30 shows the final results of inverted field data, but the point of this thesis is achieve this results know in advance that you are taken electrical measurements with the electrode array who fits better to subsurface characteristics, obtaining electrical data with good resolution and faster. Next chapter explains this process in detail.

## APPLICATION IMPROVEMENT

In this section we are going to demonstrate the aim of the project. Based on GPR results are going to create a numerical model for GPR and ERT methods and after the electrical model inversion it is going to choose the best dipole-dipole skip 0, 2, 4 or 6 configuration. Finally at the end of the process will compare the results with the obtained on the field.

First of all and based on the field GPR results we are going to raise model in GPR that try to reproduce the field data as similar as possible and extract from this model the values for the ERT modeling. In Figure 32, and after several tests, we observe that this model match good with the original data. For the modeling it has reproduced the model with topography but in order to see it better, it is show the results without topography.

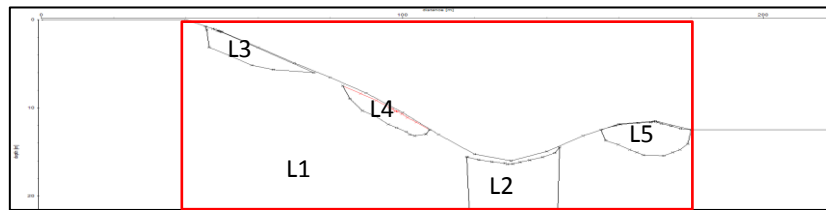


Figure 31. Raised model based on field GPR data.

In table 9 is shown the values of dielectric constant and conductivity used for the GPR forward modeling.

	$\epsilon$	$\sigma$ (S/m)	$\Omega$ (Ohm.m)
L1	10	0,0005	2000
L2	20	0,05	20
L3	5	0,00005	20000
L4	6	0,0001	10000
L5	3	0,00001	100000

Table 9. Electrical values extracted from GPR modeling.

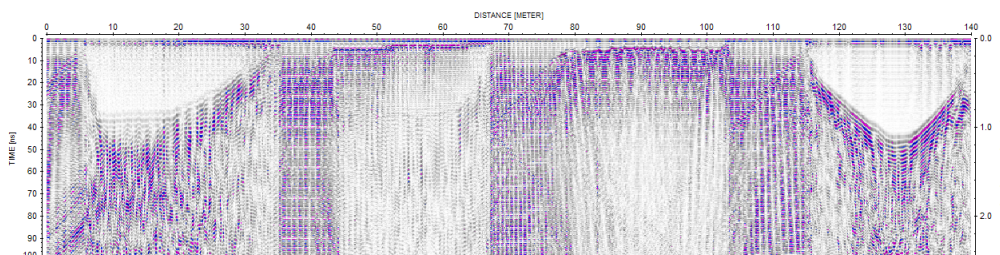


Figure 32. Radargram after forward modeling process without topography.

From the modeled radargram we can observe in a first approach five areas where the electrical properties changes. Comparing Figure 24 and Figure 32 can observe the same structures in both radargrams. In Figure 33 is shown the radargram with the buried structures highlight in red.

## The application of GPR for the modeling of ERT data and the evaluation of resolution for different electrode configurations

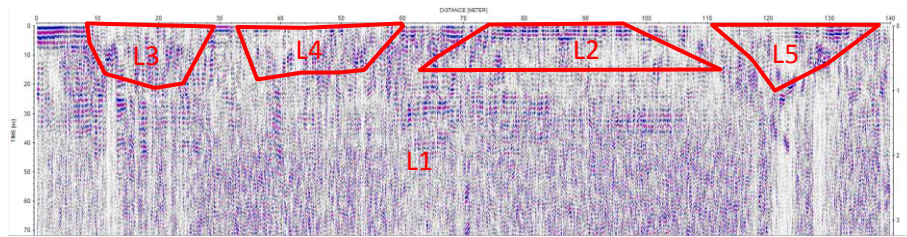


Figure 33. Radargram with highlighted structures.

The next step in the process is making the resistivity model with the values from Table 9; to do this process it has used a Matlab code which it is possible to draw the structures with the resistivity values. In the picture below it can see the raised electrical model:

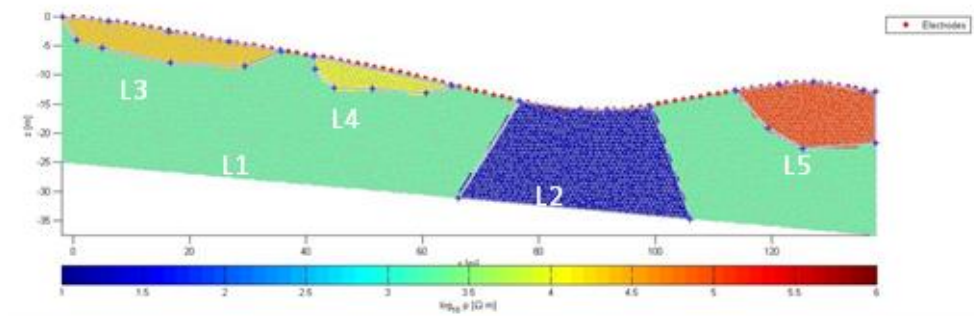


Figure 34. Numerical ERT model.

After the Matlab algorithm it has to model the resistances for the appropriate array configuration; to do this process it has used the software CRMod to obtain the resistances of the model. CRMod generates a text file ready to invert with the software CR Tomo.

Afterward it is going to check which array configuration is better to solve this raised model, to arrange this it has checked the Dipole-Dipole skip 0, 2, 4, 6 configurations. The selected array configuration is Dipole-Dipole instead others, like Wenner, because it is expected more detailed profiles and with the Dipole-Dipole can collect more number of data point and generate a more detailed profiles. In Figure 35 it can see the results after the inversion of results.

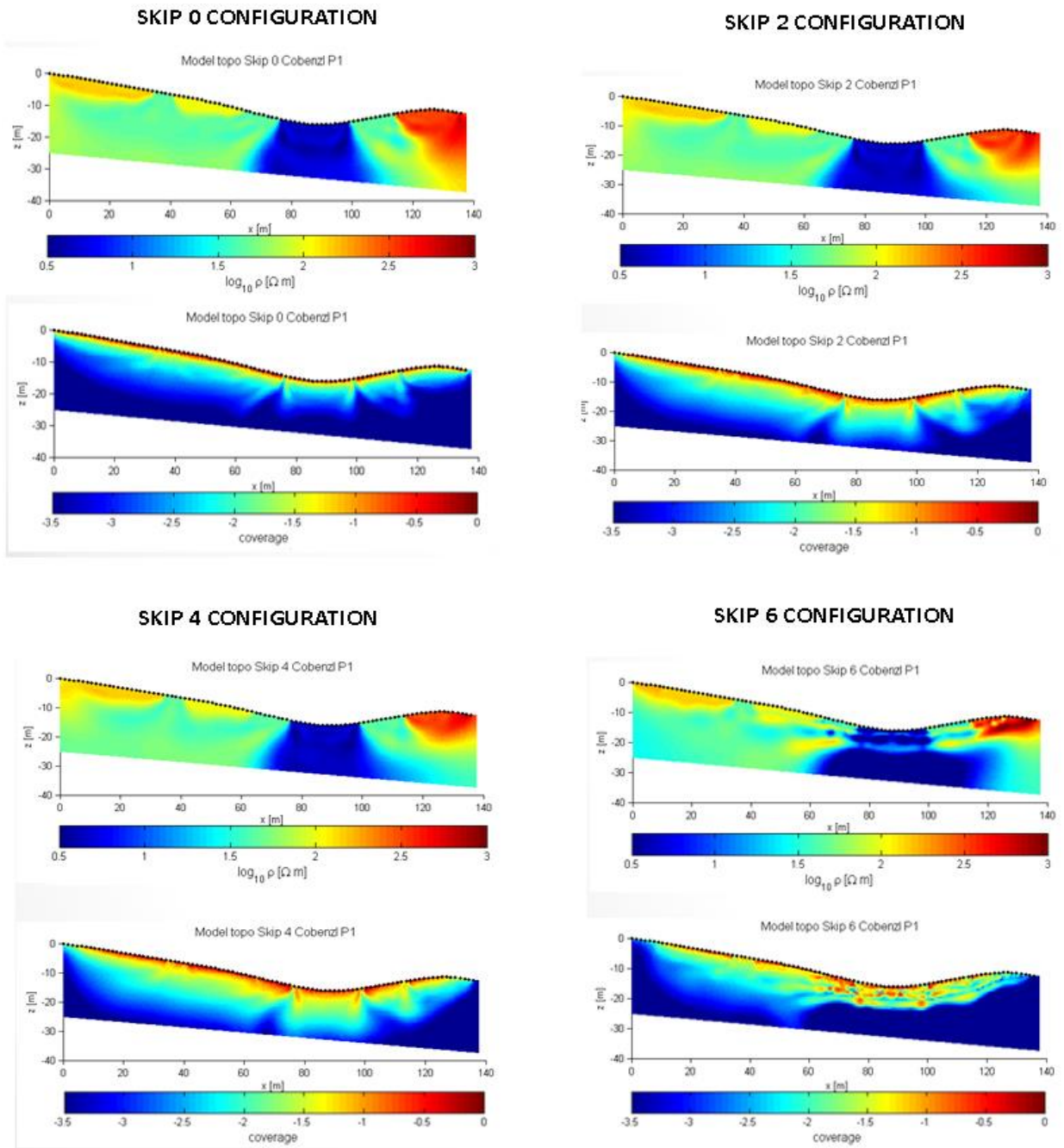


Figure 35. Comparing of different Dipole-Dipole skip configuration results.

In a detailed analysis of the results it can observe that in Skip 0 configuration the structures are clear and well defined, but observing the sensitivity model it can see that this model has a very shallow sensitivity, between 3 or 8 meters. The Skip 2 and 4 results are very similar in the structure model, but in the sensitivity part the Skip 4 go deeper. The Skip 6 does not work very well, it can see how the structures diffuse and the sensitivity model is very anomalous.

## The application of GPR for the modeling of ERT data and the evaluation of resolution for different electrode configurations

After this first analysis it can observe that the Skip 2 and Skip 4 are the best configurations to solve the raised complex model, but going forward it has to choose the better of those two configurations, and that is the Skip 4 because it has less number of data points, so we can measure quickly with a good results in inversion process.

Finally, in Figure 36, we can observe how similar are the field data results compare with the inverted model data.

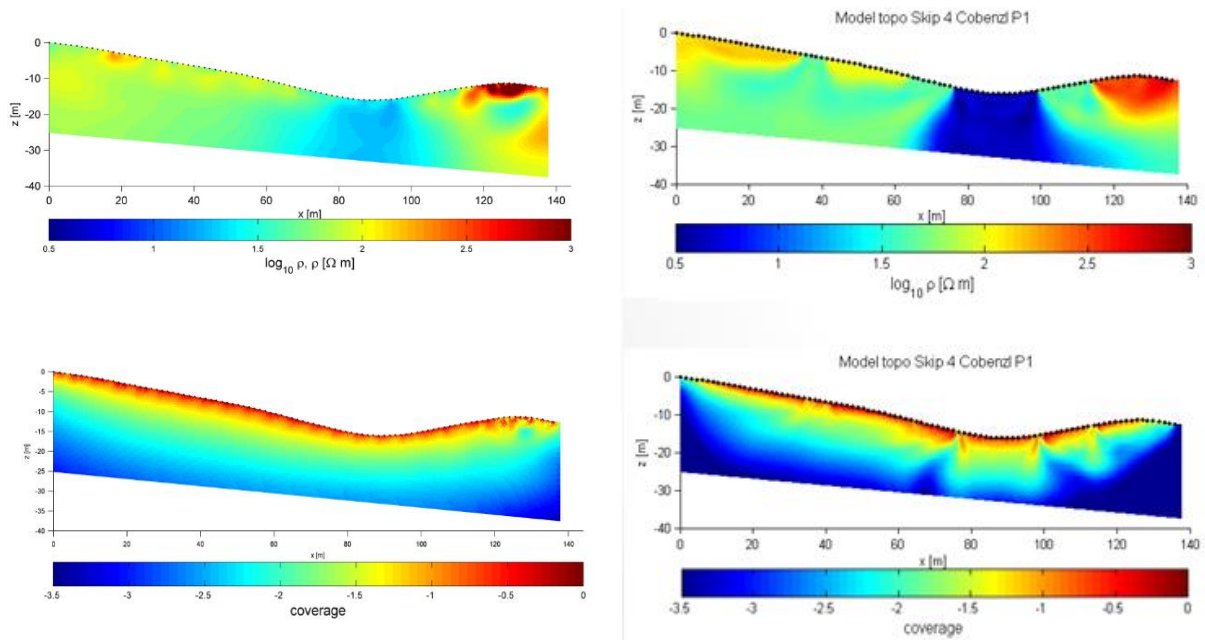


Figure 36. Comparing of different Dipole-Dipole skip configuration results.

## CONCLUSIONS

In conclusion after all exposed it can state the following ideas:

- It has been demonstrated that modeling is necessary to know in advance which is the response of different kind of subsurface.
- Has been demonstrated that the use of GPR results to choose the best array configuration to take ERT measurements is better than take ERT measurements without any previous information.
- Has been verified with real field data that the use of GPR results to improve the ERT array configuration generates results that, supported by a numerical model, are very similar.
- GPR is a fast method to obtain a first image of shallow subsurface and helps with the decision of which array take ERT measurements.
- Using both techniques combined over a single method improve the imaging results.

## BIBLIOGRAPHY

- [1] Telford, W. M., Geldart, L. P., Sheriff, R. E. (1990). Electrical properties of rocks and minerals. Applied Geophysics Second Edition. (283-292).
- [2] Telford, W. M., Geldart, L. P., Sheriff, R. E. (1990). Resistivity Methods. Applied Geophysics Second Edition. (522-577).
- [3] Annan, A. P. (2003). Ground Penetrating Radar. Principles, procedures and applications. (43-47,)
- [4] Everett, M. E. (2013) Near-Surface Applied Geophysics. (239-250)
- [5] Sandmeier K. J. (1993) Reflexw manual. (229-340)
- [6] H. W. Chen, T. M. Huangr. (1998) Journal of Applied Geophysics 40 139–163
- [7] Lampe, B. Holliger, K. Green, A. G. (2003) A finite-difference time-domain simulation tool for ground penetrating radar antennas. (971-987)
- [8] Sandmeier scientific software. [www.sandmeier-geo.de/reflexw.html](http://www.sandmeier-geo.de/reflexw.html)
- [9] Binley, A. Kemna, A. (2005) DC Resistivity and induced polarization methods. (129-154)
- [10] Kemna, A. (2000) Tomographic Inversion of complex resistivity. (58-71)